2346–2354 *Nucleic Acids Research, 2010, Vol. 38, No. 7* *Published online 15 January 2010*
doi:10.1093/nar/gkp1251

Anatomy of mouse recombination hot spots

Zhen K. Wu, Irina V. Getun and Philippe R. J. Bois*

Genome Plasticity Laboratory, Department of Cancer Biology, The Scripps Research Institute, Scripps Florida, Jupiter, FL 33458, USA

Received November 30, 2009; Revised December 21, 2009; Accepted December 27, 2009

ABSTRACT

Genome-wide analyses have suggested thousands of meiotic recombination hot spots across mammalian genomes. However, very few hot spots have been directly analyzed at a sub-kb scale for crossover (CO) activity. Using recombinant inbred strains as a CO library, here we report the identification and detailed characterization of seven new meiotic hot spots on mouse chromosome 19, more than doubling the number of currently available mouse hot spots. Although a shared feature is the narrow 1.5–2.5-kb width of these recombinogenic sites, these analyses revealed that hot spots have diverse sequence attributes and distinct symmetric and asymmetric CO profiles. Interestingly, CO molecules with discontinuous conversion tracts are commonly observed, contrasting with those found in human. Furthermore, unlike human hot spots, those present in the mouse do not necessarily have a quasi-normal CO distribution but harbor CO repulsion zones within recombinogenic cores. We propose a model where local chromatin landscape directs these repulsion zones.

INTRODUCTION

Crossover (CO) events that occur during meiotic recombination are necessary for proper formation of gametes and for generating diversity. A peculiarity of meiosis is the programmed nature of double-strand breaks (DSBs), which are induced by the conserved meiotic endonuclease Spo11 (1,2). Interestingly, recombination is not random but rather concentrates in permissive regions coined hot spots (3). However, the mechanisms that direct DSB to these hot spots, which represent only 1–2% of mammalian genomes, are poorly understood. Data from multiple model systems suggests that a combination of primary sequence (4,5), higher-order chromosome structure (6,7), chromatin accessibility (8,9) and a possible histone code (10–13) may generate a preferred environment for Spo11-directed DSB.

Using linkage disequilibrium, sperm DNA and one-generation recombination typing analyses, studies in human and mice have established that recombination hot spots are generally spaced 50- to 100-kb apart with width of 1- to 2-kb (14–18). Surprisingly, although the mouse provides the ideal model for defining the rules and mechanisms regulating DSB initiation and repair in higher eukaryotes, only a few mouse recombination hot spots have been characterized in detail and directly analyzed for CO activity (17,19–21). Moreover, most studies have focused on the highly active *Psmb9* hot spot that has a recombination frequency (RF) of 1.1% (22). Such extreme hot spots represent less than 2% of all recombinogenic loci (17), and may have very unique characteristics when compared to the majority of hot spots that have peak RFs of 10^{-3} to 10^{-5} (23–26).

Using recombinant inbred (RI) mouse strains as a CO library, we now report seven new recombinogenic loci along chromosome (chr) 19, more than doubling the current catalog of mouse recombination hot spots. Detailed analyses of their sequences and CO profiles revealed a remarkable diversity. This panel of mouse recombination hot spots provides a valuable resource to understand the genomic environment favorable for Spo11-driven DSB initiation, to explore the repair mechanisms leading to CO and non-crossover (NCO) molecules, and to define factors that contribute to evolutionary turnover of mammalian hot spots.

MATERIALS AND METHODS

Mouse strains

Mice used in this study were bred and maintained at the Animal Resource Center facility of The Scripps Research Institute—Scripps Florida under the Institutional Animal Care and Use Committee guidelines and approved protocol. Mice strains C57Bl/6J (stock# 664), DBA/2J (stock# 671) and C57Bl/6JxDBA/2J F1 males (B6D2F1/J, stock# 100006) were purchased from the Jackson

*To whom correspondence should be addressed. Tel: +1 561 228 3208; Fax: +1 561 228 3056; Email: pbois@scripps.edu

Laboratory (Bar Harbor, ME). Additional crosses were generated in the Scripps Florida Animal Research Center.

CO identification

The first 36 DNAs of the BXD recombinant inbred lines (BXD1 to BXD42) were purchased from the Jackson Laboratory DNA resource (Bar Harbor, ME). CO localizations were restricted to mouse chromosome 19. The high density BXD RI strain distribution patterns (~11 500 genomic locations and 211 on chromosome 19 alone) available on the Mouse Phenome Database (MPD) single nucleotide polymorphisms (SNPs; www.jax.org/phenome/SNP) were used as a starting point. The average distance between typed SNPs along chromosome 19 was 220-kb (136-kb median). We combined these chromosome maps with the available C57Bl/6J and DBA/2J dense SNP maps obtained from the same source. This allowed us to focus on the most polymorphic regions between the two strains (Figure 1 and Supplementary Table S1). Narrowing CO intervals of selected regions were performed using SNPs available in the MPD SNPs database in the BXD RI DNA of interest (55 145 SNPs for chr 19 alone with an average of one SNP per kb). Once a 10- to 15-kb interval was reached, the entire region was sequenced (DBA/2J and BXD RI studied) to identify all polymorphisms. Most oligonucleotides (Sigma, St Louis, MO) were designed in unique genomic regions using the Primer3 web-software interface (frodo.wi.mit.edu/primer3/) as described (20). Repeats were identified using the RepeatMasker web-software (www.repeatmasker.org/cgi-bin/WEB RepeatMasker). A complete description of the oligomers and PCR conditions used can be found in the Supplementary Data (Supplementary Tables S2 and S3). Additional oligomer sequences are available upon request.

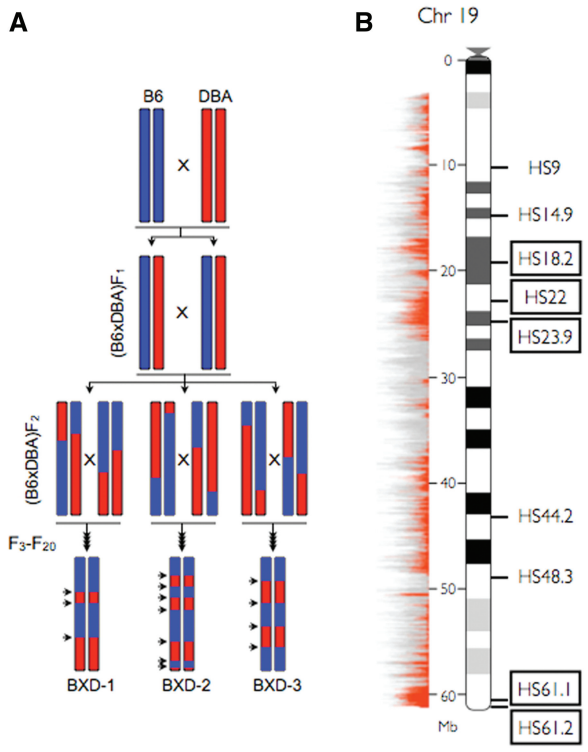

Figure 1. Strategy used to identify recombination hot spots using recombinant inbred panels. (**A**) Depiction of the breeding scheme used to generate recombinant inbred strains, here C57Bl/6J (B6, blue) crossed with DBA/2J (DBA, red, adapted from ref. 20). (**B**) A schematic of mouse chromosome 19 is shown together with the SNP density between both strains. Grey bars indicate the position and numbers of SNPs for C57Bl/6J and the 15 other high-density strains present in the Mouse Phenome SNP Database. The SNP locations where C57Bl/6J and DBA/2J are polymorphic are indicated in red. HS9 and HS22 were previously identified (20). Boxed numbers indicate highly polymorphic hot spots.

Sperm DNA extraction, quantification and CO analyses

DNA extraction and quantification were performed as described (20). Allele-specific oligomers (ASOs) were designed empirically and optimal annealing temperature was determined using a gradient PCR block (Eppendorf Mastercycler), by amplifying either a 1:1 ratio mix of C57Bl/6J and DBA/2J DNA as a negative control and the BXD RI strain DNA where the CO was located as a positive control (BXD16 and 33 for HS14.9, BXD1 for HS18.2, BXD35 for HS23.9, BXD28 for HS44.2, BXD36 for HS48.3, BXD16 for HS61.1 and BXD27 for HS61.2). The ASO sequences and PCR conditions used to detect COs in both orientations are provided in Supplementary Tables S2 and S3. The overall strategy consisted of two rounds of ASO amplification (Figure 2) as described (20). DNA inputs per small-pool PCR reaction were equivalent to an expected 0.3 recombinant

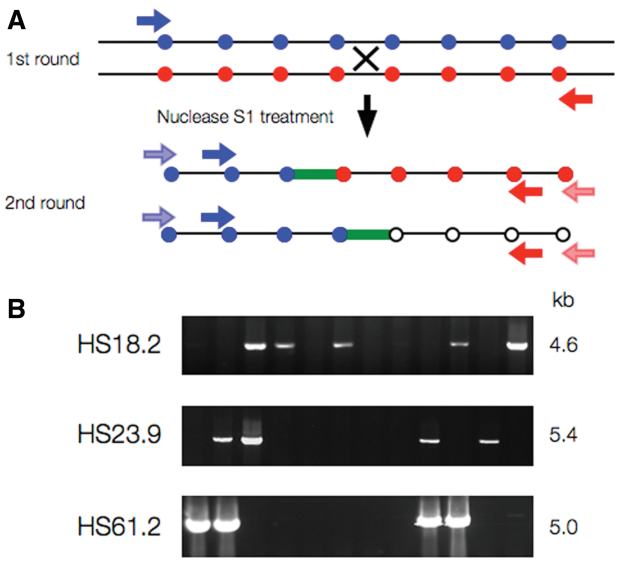

Figure 2. The isolation of meiotic-specific recombinant molecules. (**A**) Sperm DNA from C57Bl/6JxDBA/2J F1 mouse was amplified across the recombinogenic active region using two PCR rounds of nested allele-specific oligonucleotide (ASO) pairs. Primers are indicated with arrows, polymorphisms with blue and red circles and the CO interval shown in green. S1 nuclease treatment removes any single-stranded DNA that could generate jump-PCR artifacts [schematic adapted from (20)]. (**B**) Representative small-pool PCR recombination detection assays (12 reactions) are shown at three different hot spots as indicated. The final fragment size is provided.

molecules per pool and consisted of ~4000 amplifiable molecules for HS14.9, 2000 for HS18.2, 10 000 for HS23.9, 1000 for HS44.2, 15 000 for HS48.3, 500 for HS61.1 and 500 for HS61.2. We typically obtained 15–30% positive pools per experiment, to limit the frequency of reactions with two recombinant molecules. Each recombinant molecule was sequenced and analyzed using the Sequencher software (v4.9, GeneCodes).

RESULTS

Identification of recombination hot spots on mouse chromosome 19

We used the BXD RI panel as a CO library to identify meiotic recombination hot spots on mouse chr 19, where individual CO sites identified by genotyping of the RI lines are indicative of potential recombination hot spots (20). Indeed, the vast majority of mammalian COs take place within hot spots (3). The PCR-based strategy we developed allows for the efficient detection of recombinant molecules exclusively in sperm DNA, thus confirming the *bona fide* nature of these meiotic recombination hot spots (Figures 1 and 2, see also 'Materials and methods' section). To identify hot spots in the BXD RI panel having suitable polymorphisms that would allow for detailed CO analyses, we focused on the most polymorphic regions present in the Mouse Phenome SNP Database (www.jax.org/phenome/SNP). We initially surveyed all 58 COs of the 36 BXD RI strains along chr 19 (Supplementary Figure S1 and Table S1). However, with an average of approximately one SNP per kb along chr 19 (55 145 SNPs for the 61.3-Mb-long chr 19), only 15 of these 58 COs were in sufficiently polymorphic regions, and after narrowing the CO interval only seven were divergent enough to provide detailed informative CO profiles (Figures 3 and Supplementary Figure S1). With an expected hot spot width of 1.5–2.5 kb, we set an arbitrary cut-off of at least three SNPs across the CO interval. Sequencing the final 8–10 kb for each of these sites revealed large numbers of new SNPs not present in the database. This was surprising, since sequencing of 109 sites containing at least one known SNP, to narrow the various CO intervals of our initial 15 targets, uncovered only 28 new polymorphisms (21 SNP and seven indels) out of the expected 169 documented in the SNP database (12.5% new polymorphisms). However, in the last 4–5-kb regions that encompassed recombination hot spots, we observed a 200% increase in new polymorphisms. Indeed, where only 84 SNPs were expected we identified an additional 170 polymorphisms (114 SNPs and 56 indels). Thus, these recombinogenic loci had, on average, an 8-fold increase in new polymorphisms versus non hot spot sequences (170 new SNPs for 32-kb scanned versus 28 new SNPs for 43-kb sequenced, respectively).

Analysis of the genomic locations of the identified recombination hot spots revealed that DSB are initiated in diverse environments (Figure 3). Indeed, hot spots were found across exons (HS44.2 *Pkd211 Ex12-14*), within transcribed regions (HS23.9 *Apba1*, HS48.3 *Sorcs3*, HS61.1 *Grk5*), or in coding deserts of the genome (HS14.9, HS18.2, HS61.2). In addition, GC-content and GC-skew analyses did not reveal any specific patterns within the 20 kb immediately surrounding these hot spots (Supplementary Figures S2 and S3). Interspersed repeats and low complexity DNA sequences analysis also failed to reveal any preferred elements within or near recombination hot spots. In contrast, remarkable diversity in such elements was observed at recombinogenic loci where the sub-telomeric HS61.2 locus exclusively harbors LTR repeats whereas HS9 only has juxtaposed SINE/LINE elements (Figure 1 and Supplementary Table S4). We conclude that the initiation of DSB by Spo11 is permissive to a wide array of genomic environments.

CO profile analyses

For each of the final seven hot spots, we developed allele-specific PCR strategies to identify recombinant molecules in both orientations (Table 1, Supplementary Tables S2 and S3) and confirmed their true recombinogenic nature by analyzing F1 male offspring from DBA/2J crossed with C57Bl/6J mice. These assays confirm the *bona fide* recombinogenic nature of these hot spots with CO rates of 0.52×10^{-4}, 1.35×10^{-4}, 0.27×10^{-4}, 2.4×10^{-4}, 0.15×10^{-4}, 5.06×10^{-4} and 5.78×10^{-4} for HS14.9, HS18.2, HS23.9, HS44.2, HS48.3, HS61.1 and HS61.2, respectively (Table 1). These seven hot spots display a 38-fold range in activity and were very comparable to the HS9, HS22 and HS37 hot spots we previously identified that have CO rates of 4.77×10^{-4}, 2.17×10^{-4} and 3.45×10^{-4}, respectively (20). None belong to the 'super' hot spot category that has recombination rates above 0.5% (27,28). Recombination frequencies were not identical between orientations at all hot spots, which most likely reflects differences in PCR efficiencies between ASO pairs, as previously observed (19,20).

Complete sequencing of all recombinant molecules at each of the seven hot spots defined their recombination profiles in both orientations (Figure 4). These analyses revealed all possible scenarios, with both neutral (HS14.9, HS48.3 and HS61.1) and asymmetric (HS18.2, HS23.9, HS44.2 and HS61.2) profiles as previously seen at mouse loci and more rarely at human sites (19,20,29). Moreover, DSB initiation asymmetry was observed for either C57Bl/6J (HS44.2 and HS61.2) or DBA/2J (HS18.2 and HS23.9) as the most active chromosome, leading to a transmission distortion that favored the weakest initiating chromosome. The relative shift between the B6-DBA and DBA-B6 were of 300, 350, 500 and 300 bp for HS18.2, HS23.9, HS44.2 and HS61.2, respectively (Figure 4). This results in over-transmission of the DBA/2J (HS44.2 and HS61.2) or the C57Bl/6J (HS18.2 and HS23.9) alleles within hot spots, where the DSB repair machinery replaces markers from the initiating chromosome, resulting in biased gene conversion that favors the donor haplotype. These observations are similar to the asymmetry seen in human (30) and mouse E_{β}, Psmb9 and HS22 CO hot spots (19,20,23).

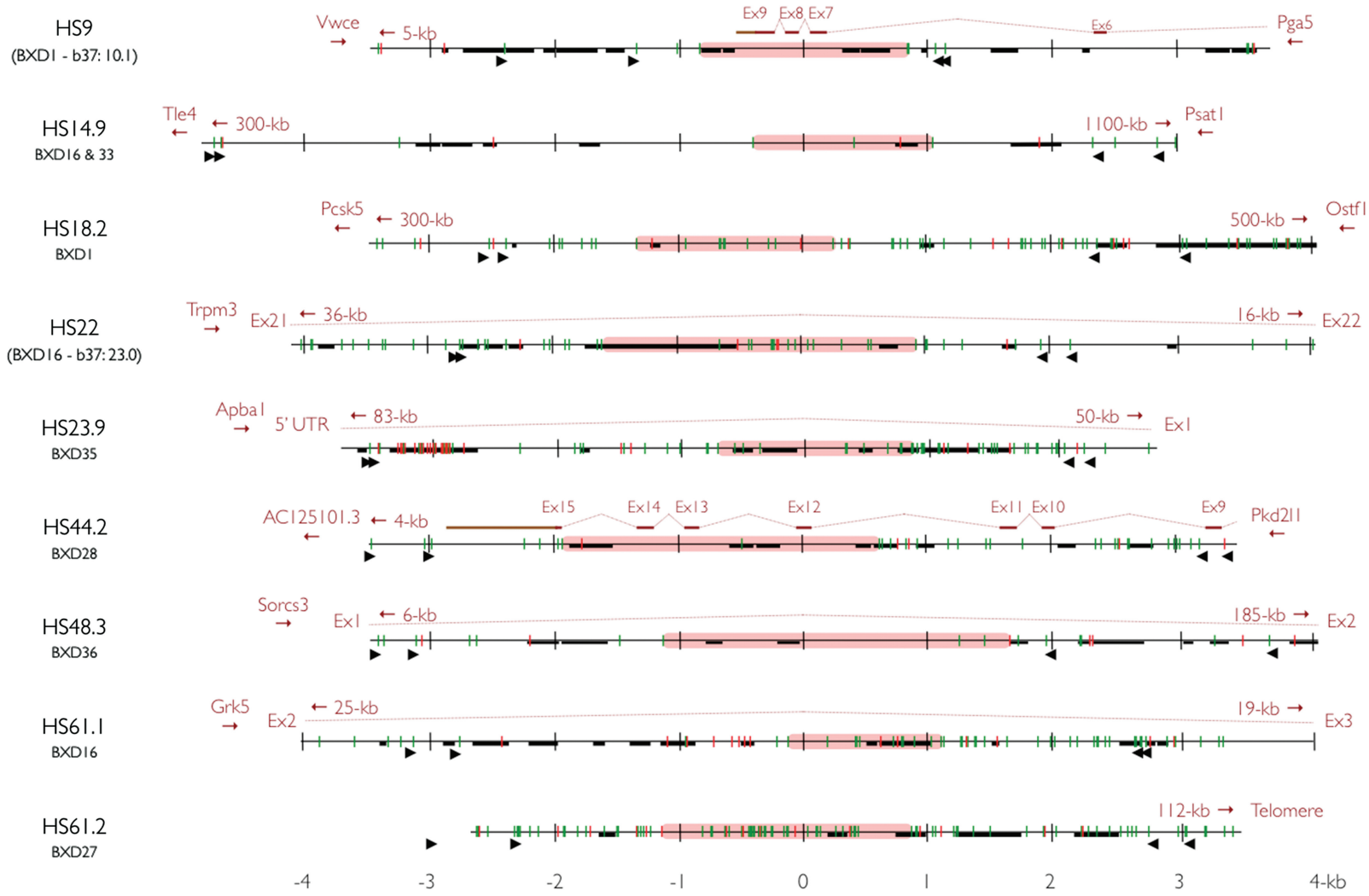

Figure 3. Genomic settings at nine mouse recombination hot spots. Details of the genomic environment found at nine chr 19 recombination hot spots are shown. HS9 and HS22 were previously identified and are shown for comparison (20). The recombinogenic core is indicated (red shade) together with the polymorphisms found between C57Bl/6J and DBA/2J strains (green vertical bars for SNPs and red for indels). Repeated elements are indicated by thicker horizontal black line (Supplementary Table S4 for complete description). Location of ASO used to detect CO molecules are shown with black arrowheads. In addition, distance and orientation from coding transcripts, gene names, exons (dark red horizontal lines) and introns (dark red dashed lines), are indicated. Orientation is centromere to the left and telomere to the right. The origin corresponds to the original CO identify in the BXD RI strains, which are indicated below the hot spot number on the left.

Table 1. Summary of sperm CO data at seven mouse recombination hot spots

Hot spot	Orientation	Number of amplifiable molecules	Number of COs detected	Rate ($\times 10^{-4}$) [95% CI]
HS14.9				
	B→D	904 226	47	0.52 [0.37–0.67]
	D→B	858 642	44	0.51 [0.36–0.66]
	Both	1 762 868	91	0.51
HS18.2				
	B→D	357 666	63	1.76 [1.33–2.20]
	D→B	472 756	59	1.25 [0.93–1.57]
	Both	830 422	122	1.47
HS23.9				
	B→D	2 328 465	81	0.35 [0.27–0.42]
	D→B	3 363 338	63	0.19 [0.14–0.23]
	Both	5 691 803	144	0.25
HS44.2				
	B→D	214 068	29	1.36 [0.86–1.85]
	D→B	121 996	42	3.44 [2.40–4.48]
	Both	336 064	71	2.11
HS48.3				
	B→D	1 870 862	45	0.24 [0.17–0.34]
	D→B	8 334 166	42	0.05 [0.04–0.07]
	Both	10 205 028	87	0.09
HS61.1				
	B→D	92 714	54	5.82 [4.27–7.38]
	D→B	111 532	48	4.30 [3.09–5.52]
	Both	204 246	102	4.99
HS61.2				
	B→D	153 370	105	6.85 [5.54–8.16]
	D→B	223 072	105	4.71 [3.81–5.61]
	Both	376 442	210	5.58

Finally, detailed CO profiles revealed domains of HS61.1 and HS61.2 that are refractory for CO resolution (Figure 4). These refractory domains have also been observed at the mouse HS22 hot spot (20). Such CO repulsion zones appear randomly positioned across hot spots, where some are found at the very center (HS22), at a boundary (the 3′ edge of HS61.1 hot spot core), or across active domains (HS61.2) of hot spot cores (Figure 4). We initially believed that this was the consequence of large insertion/deletion polymorphism, as observed at the core of the HS22 hot spot where the repulsion zone is centered on the 50-bp indel. However, there were no such polymorphisms at HS61.1 and HS61.2 that correlated with these CO repulsion zones.

Complex CO molecules are common at mouse hot spots

Complex recombinant molecules having partially repaired DNA and/or discontinuous conversion tracts were evident at the highly polymorphic HS22 hot spot (20). Given the identification of seven new recombination hot spots (Figure 3), we assessed whether such molecules were a common feature. These recombination hot spots have a gradient of complexity, from mostly simple SNPs without indels across the recombinogenic core at HS14.9 (three SNPs, 0 indel, 0.1% divergence between C57Bl/6J and DBA/2J), HS18.2 (10 SNPs, 0 indel, 0.7% divergence), HS23.9 (10 SNPs and one indel, 0.7% divergence), HS44.2 (six SNPs, two indels, 0.4% divergence) and HS48.3 (three SNPs, three indels, 0.3% divergence) to the more diverged cores at HS61.1 (14 SNPs, six indels and 2.7% divergence) and HS61.2 (36 SNPs, nine indels and 2.5% divergence).

Quite strikingly, complex molecules were evident at five out of the seven hot spots (Figure 4) and their detection directly correlates with the degree of polymorphism for these hot spots. For example, 7/102 (6.9%) and 13/210 (6.2%) CO molecules with discontinuous conversion tracts were detected at the densely polymorphic hot spots HS61.1 and HS61.2, whereas no complex molecules were observed at the HS14.9 and HS48.3 hot spots, which have few closely spaced polymorphisms across their recombinogenic domains that, we suspect, preclude the detection of short conversion patches (Figure 4 and Supplementary Figure S4). In addition, those with more intermediate polymorphism across the recombinogenic region had more modest numbers of complex CO molecules, with 2/97 (2%), 2/144 (1.4%) and 2/71 (2.8%) of such molecules at the HS18.2, HS23.9 and HS44.2 loci (one in each orientation; Figure 4 and Supplementary Figure S4), respectively.

The structure of these complex CO molecules is reminiscent of those observed at the HS22, M1 and M2 mouse hot spots (20,31), at human super hot spots [albeit at a much lower rate (28)] as well as in *Mlh1* knockout male mice (25). However, unlike at the HS22 locus, we did not detect any CO molecules containing unrepaired heteroduplex regions (20). Out of the 25 complex recombinant molecules identified, the average maximum length of the discontinuous conversion tracts was 320 bp (200 bp median). These fall in the same range as the average 217 bp maximum length (167 bp median) observed at thirteen previously identified complex molecules at the HS22 hot spot (20). When studying discontinuous conversion tract length encompassing more than one SNP (observed at HS61.1, HS61.2 and previously at HS22), we observed lengths up to a 962 bp, indicating that these molecules can be rather large. Similar molecules have also been rarely observed at human super hot spots (28). We conclude that CO molecules with discontinuous conversion tracts are a common feature of mouse meiotic recombination.

DISCUSSION

With the analyses of COs of seven new mouse recombination hot spots several features of the anatomy of mammalian hot spots are emerging. First, despite their remarkable genomic and sequence diversity, meiotic hot spots are characterized by a rather uniform width in their CO profiles, suggesting tight control in the formation and resolution of double Holliday junctions (dHJs). Second, DSB chromosome initiation bias leading to CO asymmetry and transmission distortion is commonly observed. Third, some hot spots harbor zones of CO repulsion within the recombinogenic core, suggesting that hot spots fall into two classes: those that harbor such zones of repulsion (e.g. HS22, HS61.1, HS61.2) and those that do not

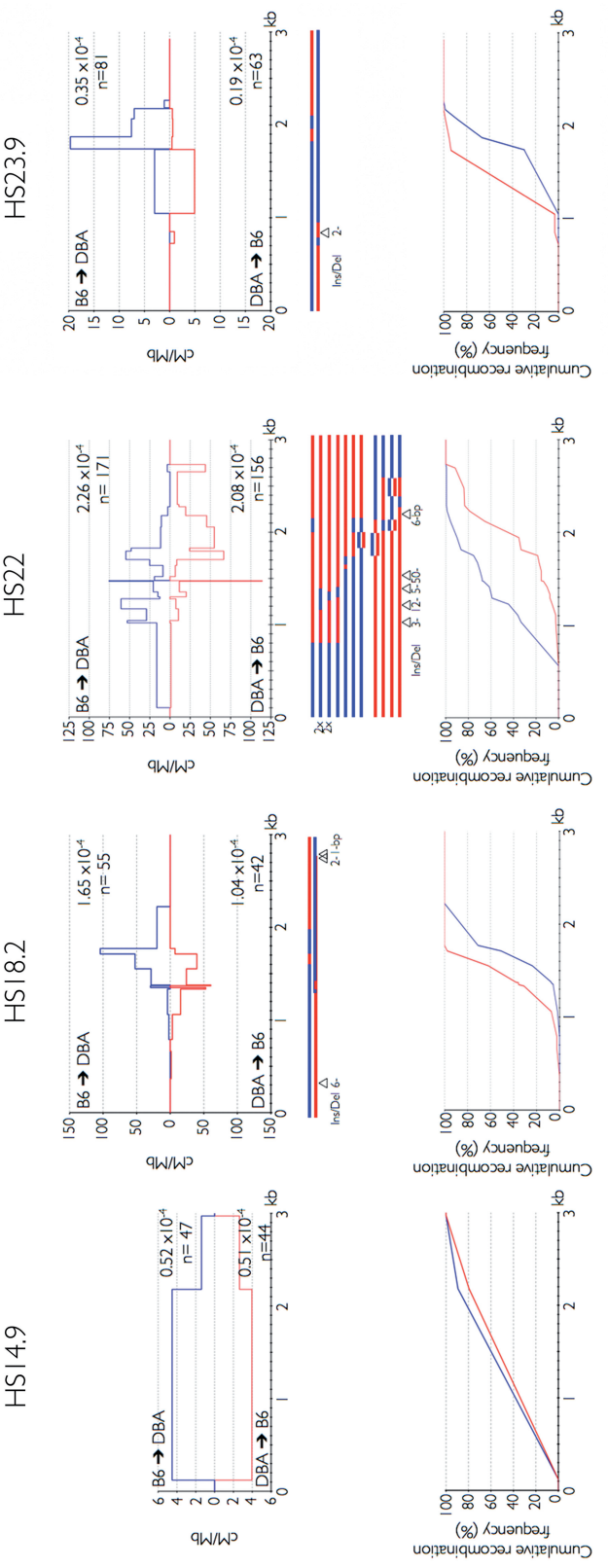

Figure 4. Hot spot CO profiles, asymmetry and the structures of complex recombinant molecules. For each hot spot the distributions of the C57Bl/6J-to-DBA/2J (blue) and DBA/2J-to-C57Bl/6J (red, as a mirror representation) CO across the central recombinogenic portion are indicated. The CO rates as well as the number of CO molecules mapped are provided. Complex structures of discontinuous conversion tract molecules are represented with blue (C57Bl/6J) and red (DBA/2J) lines. Cumulative frequencies of sperm CO in the C57Bl/6J-to-DBA/2J (blue) and DBA/2J-to-C57Bl/6J (red) orientation are shown. The HS22 profile, asymmetry and complex molecules structure have been previously reported (20) and are shown here for comparison.

(e.g. HS18.2). Finally, at least for the mouse, complex CO molecules are generated during meiotic recombination. Collectively, these findings reveal that mouse hot spots are far more diverse than those found in human or yeast (28,32).

Identification of recombination hot spots on mouse chromosome 19

A major hurdle in defining the anatomy and activity of hot spot COs is finding hot spots that harbor sufficient polymorphisms that allow detailed profile analysis. Our findings indicate that polymorphisms at recombination hot spots are under-represented by some 200% in the SNP database. While there is no definitive explanation for this rather striking discrepancy, there appears to be a bias against exhaustive SNP assignment in highly polymorphic regions of the mouse SNP database (www.jax.org/phenome/SNP). However, there is a good correlation between the number of SNPs present in the database and the number of new polymorphisms identified (Pearson correlation $r^{database\ new}_{SNP\ ,SNP} = 0.875$). The discovery of numerous new SNPs in a poorly polymorphic regions is therefore unlikely. Indeed, our most polymorphic hot spots (HS18.2, HS22, HS61.1 and HS61.2) are all located in the most polymorphic regions known between C57Bl/6J and DBA/2J (Figure 1B).

The genomic diversity observed at all mouse hot spots (Figure 3) is similar to that observed in the human genome from the HapMap project (16,33). We did not identify hot spots in the promoter regions of any genes, which distinguishes mammalian hot spots from those found in yeast (34). Although the numbers of mouse hot spots thus far characterized at high resolution precludes the identification of any 'hot spot' motif, three of the hot spot cores (HS22, HS44.2 and HS61.2) have the degenerate 13-mer CCNCCNTNNCCNC sequence motif that has been previously associated with recombination hot spots and genome instability in humans (35). This motif is detected at 400, 120 and 270 bp from the recombinogenic centers of HS22, HS44.2 and HS61.2, respectively. Intriguingly, the HS22 site is only present on the active C57Bl/6J chromosome. While this motif is only correlative, it may suggest that a common trans-acting factor shared between mice and human targets a subset of recombinogenic sites to render them permissive to Spo11-initiated DSB formation, in a manner akin to the *ADE6-M26* hot spot in *S. pombe* (36). Indeed, in this scenario, recombination initiation appears to be controlled by a set of histone acetyltransferase and ATP-dependent chromatin remodeling factors that alter chromatin structure (37). The precise mapping of hot spot cores to a sub-1-kb resolution using alternative methodologies, for example those defining single-strand DNA-associated DSBs (34) or Spo11-bound sequences (38), should allow the field to determine if any recurrent motif sequence is present at mouse recombination hot spots.

Insights from analyses of CO profiles

All mouse hot spots show fairly uniform widths in their recombinogenic regions, from 1.5 to 2.5 kb (Figure 4),

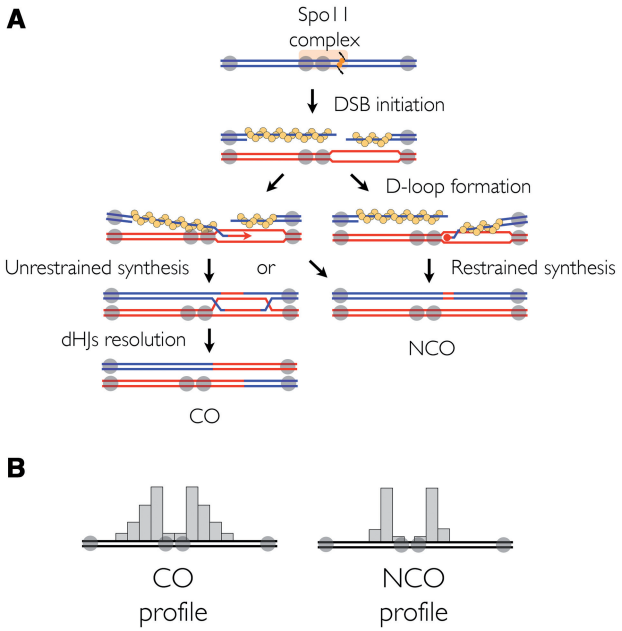

Figure 5. CO repulsion zone model at hot spot cores. (**A**) Recombination is initiated by a DSB in the vicinity of histones, which may provide a favorable environment for the Spo11 complex. Ends are resected to form single-stranded tails, which are substrates for Dmc1 and Rad51. One end forms a D-loop with its homolog and is then extended by DNA synthesis. In this model, for the right DSB end, synthesis-dependent strand annealing extension is constrained by local chromatin features (e.g. nucleosomes, DNA-binding factors indicated here with grey shaded dots), which impede D-loop extension and second end capture. Repair synthesis and ligation then forms an NCO recombinant. For the left DSB end, end extension is free of constraints and can enlarge the D-loop, allowing the second end to anneal. After annealing, repair synthesis and ligation forms a dHJ that then results in a CO. (**B**) CO repulsion zones are predicted to be occupied by chromatin-binding factors that physically impair CO across these regions. As a consequence, NCO are also expected to be observed immediately flanking these domains.

similar to previously characterized loci in mouse and human (20,21,28,31). CO asymmetry is also a rather common feature where there is a clear preference for DSB initiation from either C57Bl/6J (HS22, HS44.2, HS61.2) or DBA/2J (HS18.2, HS23.9). Asymmetry is not linked to polymorphism as it occurs in hot spots that have high (e.g. HS61.1) or low polymorphism (e.g. HS44.2).

One striking feature is the identification of CO repulsion zones located at the center (HS22), across (HS61.2), or at the periphery (HS61.1) of hot spot cores (Figure 4). Highly informative sites are necessary to obtain such detailed profiles but in three out of four cases non-uniform normal distribution profiles were observed at the same location and in both orientations. Such features are also evident in the human genome at the *C*, *G* and *J* 'super' hot spots as well as in the *MSNID* and *MSTN1a/b* loci (28,29,39). We hypothesize that the observed CO repulsion zones reflect the presence of chromatin-binding factors at the core of hot spots, which influence their resolution by directing D-loop formation of the pre-synaptic filament on the homologous chromosome (Figure 5).

Indeed, recent analysis at the *Psmb9* and *Hlx1* super hot spots indicate that histones are present at the center of at least some hot spots (13). Furthermore, the lack of any central CO repulsion zones at the HS18.2 and HS61.1 hot spots (Figure 4) suggests that chromatin organization may differ and distinguish hot spot types. Collectively, these observations support a model in which local chromatin organization (e.g. nucleosome occupancy, DNA-binding factors) has roles in promoting DSB initiation by directing Spo11 complex binding and cleavage and in forcing D-loop stabilization in one favorable orientation, with direct consequences on dHJs formation and resolution (Figure 5A). In turn, this would have direct consequences on hot spot regulation, maintenance and evolution by affecting CO and NCO profiles (Figure 5B). Indeed, the current model assumes a normal CO and NCO distribution across a given hot spot, yet our studies indicate that this does not apply to the mouse hot spots we characterized where repulsion zones in recombinogenic cores are protected from being disrupted by either CO or NCO. Such regulation would have direct consequences on hot spot evolution, where the active core of a recombinogenic locus would not be extinguished and remain active by limiting meiotic drive.

Complex CO molecules are a feature of mouse meiotic recombination

Surprisingly analyses of CO molecules generated at recombination hot spots also revealed that complex conversion tract CO molecules are quite common in the mouse (3.4%, 38 out of 1129 CO molecules analyzed). This is in stark contrast with what has been detected in human where such events are more rarely observed, with an estimated rate of 0.3% (28). We suspect that these numbers, in both cases, are underestimates, as the ability to detect such complex molecules entirely relies on SNP density. Indeed, to the best of our knowledge, no human hot spot has been described having a level of polymorphisms comparable to the hot spots found in mice. Regardless, the detection of such molecules provide indirect insights into the repair mechanisms operational following resolution of dHJs, which leaves heteroduplex DNA regions that are then repaired by the mismatch repair machinery. Specifically, the detection of discontinuous conversion tracts suggests that a patchy repair process occurs. One possibility here is that an excess of mismatch repair proteins may compete for the same template resulting in an efficient repair but with discontinuous tracts.

CONCLUSIONS

This survey has more than doubled the number of mouse meiotic recombination hot spots characterized by direct sperm analysis. Features established from previous studies revealed the extremely diverse nature of mouse recombination hot spots with the only commonality being the rather narrow 1.5–2.5-kb width (20,21,31). Indeed, we found a variety of asymmetric and symmetric CO distributions, presence of CO repulsion zones as well as quasi-normal CO profiles, generally simple CO exchanges but also discontinuous conversion tracts, and no hot spot clustering. This is in stark contrast with human hot spots, which appear far more homogeneous (28) and may reflect the genetically more homogenous nature of the population studied when compared to the laboratory mouse strains. These hot spots therefore provide a very valuable resource for exploring chromatin structure, recombination initiation and recombination intermediates in mammalian meiosis. In addition, further studies focusing on hot spot activity differences between hybrid strains should allow for detailed analyses of what determines the locale of a hot spot.

SUPPLEMENTARY DATA

Supplementary Data are available at NAR Online.

ACKNOWLEDGEMENTS

The authors are indebted to Drs J. Cleveland and T. Izard for critical comments on the manuscript and to numerous colleagues for discussions and insights. This manuscript is dedicated to Mark Hall. This is manuscript number 20432 of The Scripps Research Institute.

FUNDING

Funding for open access charges: Monies from the State of Florida to Scripps Florida.

Conflict of interest statement. None declared.

REFERENCES

1. Bergerat,A., deMassy,B., Gadelle,D., Varoutas,P.C., Nicolas,A. and Forterre,P. (1997) An atypical topoisomerase II from archaea with implications for meiotic recombination. *Nature*, **386**, 414–417.
2. Keeney,S., Giroux,C.N. and Kleckner,N. (1997) Meiosis-specific DNA double-strand breaks are catalyzed by Spo11, a member of a widely conserved protein family. *Cell*, **88**, 375–384.
3. Kauppi,L., Jeffreys,A.J. and Keeney,S. (2004) Where the crossovers are: recombination distributions in mammals. *Nat. Rev. Genet.*, **5**, 413–424.
4. Arnheim,N., Calabrese,P. and Tiemann-Boege,I. (2007) Mammalian meiotic recombination hot spots. *Annu. Rev. Genet.*, **41**, 369–399.
5. Myers,S., Spencer,C.C., Auton,A., Bottolo,L., Freeman,C., Donnelly,P. and McVean,G. (2006) The distribution and causes of meiotic recombination in the human genome. *Biochem. Soc. Trans.*, **34**, 526–530.
6. Mets,D.G. and Meyer,B.J. (2009) Condensins regulate meiotic DNA break distribution, thus crossover frequency, by controlling chromosome structure. *Cell*, **139**, 73–86.
7. Boulton,S.J. (2009) Condensin(g) crossover control to a few breaks. *Cell*, **139**, 21–23.
8. Nicolas,A. (1998) Relationship between transcription and initiation of meiotic recombination: toward chromatin accessibility. *Proc. Natl Acad. Sci. USA*, **95**, 87–89.
9. Yamada,T., Mizuno,K., Hirota,K., Kon,N., Wahls,W.P., Hartsuiker,E., Murofushi,H., Shibata,T. and Ohta,K. (2004) Roles of histone acetylation and chromatin remodeling factor in a meiotic recombination hot spot. *EMBO J.*, **23**, 1792–1803.

10. Merker,J.D., Dominska,M., Greenwell,P.W., Rinella,E., Bouck,D.C., Shibata,Y., Strahl,B.D., Mieczkowski,P. and Petes,T.D. (2008) The histone methylase Set2p and the histone deacetylase Rpd3p repress meiotic recombination at the HIS4 meiotic recombination hot spot in *Saccharomyces cerevisiae*. *DNA Rep.*, **7**, 1298–1308.
11. Borde,V., Robine,N., Lin,W., Bonfils,S., Geli,V. and Nicolas,A. (2009) Histone H3 lysine 4 trimethylation marks meiotic recombination initiation sites. *EMBO J.*, **28**, 99–111.
12. Kniewel,R. and Keeney,S. (2009) Histone methylation sets the stage for meiotic DNA breaks. *EMBO J.*, **28**, 81–83.
13. Buard,J., Barthes,P., Grey,C. and de Massy,B. (2009) Distinct histone modifications define initiation and repair of meiotic recombination in the mouse. *EMBO J.*, **28**, 2616–2624.
14. Jeffreys,A.J., Kauppi,L. and Neumann,R. (2001) Intensely punctate meiotic recombination in the class II region of the major histocompatibility complex. *Nat. Genet.*, **29**, 217–222.
15. Myers,S., Bottolo,L., Freeman,C., McVean,G. and Donnelly,P. (2005) A fine-scale map of recombination rates and hot spots across the human genome. *Science*, **310**, 321–324.
16. Frazer,K.A., Ballinger,D.G., Cox,D.R., Hinds,D.A., Stuve,L.L., Gibbs,R.A., Belmont,J.W., Boudreau,A., Hardenbol,P., Leal,S.M. *et al.* (2007) A second generation human haplotype map of over 3.1 million SNPs. *Nature*, **449**, 851–861.
17. Paigen,K., Szatkiewicz,J.P., Sawyer,K., Leahy,N., Parvanov,E.D., Ng,S.H., Graber,J.H., Broman,K.W. and Petkov,P.M. (2008) The recombinational anatomy of a mouse chromosome. *PLoS Genet.*, **4**, e1000119.
18. Chowdhury,R., Bois,P.R., Feingold,E., Sherman,S.L. and Cheung,V.G. (2009) Genetic analysis of variation in human meiotic recombination. *PLoS Genet.*, **5**, e1000648.
19. Yauk,C.L., Bois,P.R. and Jeffreys,A.J. (2003) High-resolution sperm typing of meiotic recombination in the mouse MHC Ebeta gene. *EMBO J.*, **22**, 1389–1397.
20. Bois,P.R. (2007) A highly polymorphic meiotic recombination mouse hot spot exhibits incomplete repair. *Mol. Cell. Biol.*, **27**, 7053–7062.
21. Guillon,H. and De Massy,B. (2002) An initiation site for meiotic crossing-over and gene conversion in the mouse. *Nat. Genet.*, **32**, 296–299.
22. Shiroishi,T., Hanzawa,N., Sagai,T., Ishiura,M., Gojobori,T., Steinmetz,M. and Moriwaki,K. (1990) Recombinational hot spot specific to female meiosis in the mouse major histocompatibility complex. *Immunogenetics*, **31**, 79–88.
23. Baudat,F. and de Massy,B. (2007) Cis- and trans-acting elements regulate the mouse Psmb9 meiotic recombination hot spot. *PLoS Genet.*, **3**, e100.
24. Grey,C., Baudat,F. and de Massy,B. (2009) Genome-wide control of the distribution of meiotic recombination. *PLoS Biol.*, **7**, e35.
25. Guillon,H., Baudat,F., Grey,C., Liskay,R.M. and de Massy,B. (2005) Crossover and noncrossover pathways in mouse meiosis. *Mol. Cell*, **20**, 563–573.
26. Parvanov,E.D., Ng,S.H., Petkov,P.M. and Paigen,K. (2009) Trans-regulation of mouse meiotic recombination hot spots by Rcr1. *PLoS Biol.*, **7**, e36.
27. Mizuno,K., Koide,T., Sagai,T., Moriwaki,K. and Shiroishi,T. (1996) Molecular analysis of a recombinational hot spot adjacent to Lmp2 gene in the mouse MHC: fine location and chromatin structure. *Mamm. Genome*, **7**, 490–496.
28. Webb,A.J., Berg,I.L. and Jeffreys,A. (2008) Sperm cross-over activity in regions of the human genome showing extreme breakdown of marker association. *Proc. Natl Acad. Sci. USA*, **105**, 10471–10476.
29. Jeffreys,A.J. and Neumann,R. (2005) Factors influencing recombination frequency and distribution in a human meiotic crossover hot spot. *Hum. Mol. Genet.*, **14**, 2277–2287.
30. Jeffreys,A.J. and Neumann,R. (2002) Reciprocal crossover asymmetry and meiotic drive in a human recombination hot spot. *Nat. Genet.*, **31**, 267–271.
31. Kauppi,L., Jasin,M. and Keeney,S. (2007) Meiotic crossover hot spots contained in haplotype block boundaries of the mouse genome. *Proc. Natl Acad. Sci. USA*, **104**, 13396–13401.
32. Robine,N., Uematsu,N., Amiot,F., Gidrol,X., Barillot,E., Nicolas,A. and Borde,V. (2007) Genome-wide redistribution of meiotic double-strand breaks in Saccharomyces cerevisiae. *Mol. Cell. Biol.*, **27**, 1868–1880.
33. The International HapMap Consortium. (2005) A haplotype map of the human genome. *Nature*, **437**, 1299–1320.
34. Buhler,C., Borde,V. and Lichten,M. (2007) Mapping meiotic single-strand DNA reveals a new landscape of DNA double-strand breaks in Saccharomyces cerevisiae. *PLoS Biol.*, **5**, e324.
35. Myers,S., Freeman,C., Auton,A., Donnelly,P. and McVean,G. (2008) A common sequence motif associated with recombination hot spots and genome instability in humans. *Nat. Genet*, **5**, e324.
36. Kon,N., Krawchuk,M.D., Warren,B.G., Smith,G.R. and Wahls,W.P. (1997) Transcription factor Mts1/Mts2 (Atf1/Pcr1, Gad7/Pcr1) activates the M26 meiotic recombination hot spot in Schizosaccharomyces pombe. *Proc. Natl Acad. Sci. USA*, **94**, 13765–13770.
37. Hirota,K., Mizuno,K., Shibata,T. and Ohta,K. (2008) Distinct chromatin modulators regulate the formation of accessible and repressive chromatin at the fission yeast recombination hot spot ade6-M26. *Mol. Biol. Cell*, **19**, 1162–1173.
38. Neale,M.J., Pan,J. and Keeney,S. (2005) Endonucleolytic processing of covalent protein-linked DNA double-strand breaks. *Nature*, **436**, 1053–1057.
39. Neumann,R. and Jeffreys,A.J. (2006) Polymorphism in the activity of human crossover hot spots independent of local DNA sequence variation. *Hum. Mol. Genet.*, **15**, 1401–1411.